# Implementation of a Modified Moving Least Squares Approximation for Predicting Soft Tissue Deformation using a Meshless Method

**Habibullah Amin Chowdhury[a], Grand Roman Joldes[a], Adam Wittek[a], Barry Doyle[a], Elena Pasternak[b] and Karol Miller[a]**

[a]Intelligent Systems for Medicine Laboratory (ISML), The University of Western Australia.

[b]School of Mechanical and Chemical Engineering, The University of Western Australia.

**Abstract** In applications where the organic soft tissue undergoes large deformations, traditional finite element methods can fail due to element distortion. In this context, meshless methods, which require no mesh for defining the interpolation field, can offer stable solutions. In meshless methods, the moving least square (MLS) shape functions have been widely used for approximating the unknown field functions using the scattered field nodes. However, the classical MLS places strict requirements on the nodal distributions inside the support domain in order to maintain the non-singularity of the moment matrix. These limitations are preventing the practical use of higher order polynomial bases in classical MLS for randomly distributed nodes despite their capability for more accurate approximation of complex deformation fields. A modified moving least squares (MMLS) approximation has been recently developed by ISML. This paper assesses the interpolation capabilities of the MMLS. The proposed meshless method based on MMLS is used for computing the extension of a soft tissue sample and for a brain deformation simulation in 2D. The results are compared with the commercial finite element software ABAQUS. The simulation results demonstrate the superior performance of the MMLS over classical MLS with linear basis functions in terms of accuracy of the solution.

## 1 Introduction

In case of brain surgery simulation, our vision is to enable a surgeon to interact with the computing facilities in the operating theatre and to visualize the results in real-time with high accuracy. In this way, a surgeon, without requiring any expert knowledge in numerical computation, would be able to evaluate the implications of each stage of a surgical procedure and explore potential alternative solutions. For this purpose, a robust and accurate method for solving the fundamental equations describing the biomechanical behaviour of the subject is an essential requirement. Conventionally, this kind of real-time computation in

biomechanics depends on linear finite element algorithms which assume infinitesimal deformations [1, 2]. However, modelling of the brain for applications such as neurosurgical simulation and neuroimage registration for image-guided surgery is a nonlinear problem of continuum mechanics which involves large deformations and large strains with geometric and material nonlinearities. Therefore the infinitesimal assumption is not satisfied where such large deformations occur. Furthermore, in such cases, finite element methods can fail due to element distortion. In this context, meshless methods [3, 4] provide a better alternative. The complex finite element grid generation and element distortion problems are avoided, as only a cloud of points are required for discretising the model [5, 6] in meshless methods; a predefined mesh is not necessary. The meshless shape functions are important in approximating the unknown field functions to find the approximate solution to a problem governed by PDEs and boundary conditions using these arbitrarily distributed field nodes [4]. The Moving Least Squares (MLS) shape functions have been preferred predominantly in meshless methods [3, 7] due to the smoothness, continuity and consistency of the approximation field they create.

The MLS method was first introduced by Shepard [8] to construct smooth approximations for fitting a cloud of points [9]. In 1981, Lancaster and Salkauskas [10] extended this method for general surface generation problems. In generating meshless shape functions, higher order polynomial basis functions are useful in approximating complex data distributions. They also have the potential to increase the accuracy of the simulation results compared with linear basis function. However, as the degree of polynomial basis is increased, more nodes need to be included in the support domain to be able to compute the shape functions. Consequently, the size of the support domain gets enlarged resulting in increased computational cost for a given discretisation. Furthermore, not all node distributions can be used in numerical computation for a given size of the support domain. Nevertheless, in most cases, a valid or “admissible” node distribution can be achieved by increasing the support domain size, which is often controlled by a dilatation parameter [11]. In this context, Joldes et al. [12] has recently presented a modified MLS approximation which allows higher order polynomial basis functions to be used under the same conditions as lower degree basis functions. Such an approximation can be used to create a more accurate meshless method without the need to change the nodal distribution or dilatation parameters used.

This paper focuses on the evaluation of a meshless method based on the modified MLS (MMLS) shape function developed by Joldes et al. [12] in two specific cases of biomechanics simulations: extension of a soft tissue sample and simulation of a craniotomy induced brain shift. A comparison between the MMLS and the classical MLS with linear and quadratic basis in approximating a bivariate function is also presented.

## 2 The Modified Moving Least Squares Method

The procedure for constructing classical MLS shape function starts with the approximation of a function $u$(x), denoted by $u^h$(x), which is defined by a combination of $m$ monomials (also called basis functions) [4].

$$u^h(\mathbf{x}) = \sum_{i=1}^{m} p_i(\mathbf{x}) a_i(\mathbf{x}) = \mathbf{p}^T(\mathbf{x})\boldsymbol{a}(\mathbf{x}) \quad (1)$$

where $m$ is the number of terms in the basis $\mathbf{p}(\mathbf{x})$, and $a_i(\mathbf{x})$ are coefficients that depend on the spatial coordinates $\mathbf{x}$. These coefficients are computed by minimizing an error functional defined based on the weighted least squares errors:

$$J(\mathbf{x}) = \sum_{j=1}^{n}[\left(u^h(\mathbf{x}_j) - u_j\right)^2 w(\|\mathbf{x} - \mathbf{x}_j\|)] \quad (2)$$

where $n$ is the number of nodes in the support domain of $\mathbf{x}$. Rewriting in matrix form yields:

$$\mathbf{J} = \mathbf{(Pa - u)}^T\mathbf{W(Pa - u)} \quad (3)$$

Minimization is done by setting the partial derivatives of the error functional $\mathbf{J}$ to zero:

$$\frac{\partial \mathbf{J}}{\partial \mathbf{a}} = \mathbf{P}^T\mathbf{WPa(x)} - \mathbf{P}^T\mathbf{Wu} = 0 \quad (4)$$

Finally, by solving the resulting system of equations, the MLS approximation is obtained as

$$u^h(\mathbf{x}) = \sum_{j=1}^{n} \emptyset_j(\mathbf{x}) u_j = \boldsymbol{\Phi}^{\boldsymbol{T}}(\mathbf{x})\mathbf{u} \quad (5)$$

where

$$\emptyset_j(\mathbf{x}) = p^T(\mathbf{x})(\boldsymbol{M}^{(-1)}(\mathbf{x})\boldsymbol{B}(\mathbf{x})) \quad (6)$$

$$\boldsymbol{M}(\mathbf{x}) = \sum_{j=1}^{n} w(\mathbf{x} - \mathbf{x}_j) p(\mathbf{x}_j) p^T(\mathbf{x}_j) \quad (7)$$

$$\boldsymbol{B}(\mathbf{x}) = [B(\mathbf{x}_1) \quad B(\mathbf{x}_2) \ \ldots \ B(\mathbf{x}_n)] \quad (8)$$

$$B(\mathbf{x}_1) = w(\mathbf{x} - \mathbf{x}_1) p(\mathbf{x}_1) \quad (9)$$

Here, $\mathbf{u}$ is the nodal vector parameters of all the nodal field variables in the local support domain, $\boldsymbol{\Phi}(\mathbf{x})$ is the vector of MLS shape functions and $\boldsymbol{M}(\mathbf{x})$ is known as the moment matrix. Generally, linear or quadratic basis functions and cubic or quartic weight functions are used to create the approximation.

As can be seen from equation (6), the shape functions construction depends on the non-singularity of the moment matrix defined by equation (7). The necessary conditions for the moment matrix to be non-singular depend on the types of basis functions used. For example, in a two-dimensional case, the moment matrix is non-singular as long as there are at least 3 non-collinear nodes in the support domain for linear basis functions; whereas for a quadratic basis, at least 6 nodes are needed in the support domain. The support domain of a point **x** determines the number of nodes used to compute the approximation value at **x**. However, some nodal distributions can still lead to singular moment matrices even if enough nodes are included in the support domain. This type of scenario can occur, for example, if the nodes are distributed on two parallel lines in 2D. To overcome this problem, the traditional remedy is to enlarge the support domains in order to include more nodes. This, however, leads to higher approximation error and increased computational cost due to the more linearly dependent shape functions in the local area. Consequently, these limitations prevent the practical use of higher order polynomial basis for randomly distributed nodes despite their potential capability for better approximation of complex deformation fields and better convergence properties.

In this context, Joldes et al. [12] developed a modified MLS with second order polynomial basis. The development of MMLS is based on the observation that a singular moment matrix mainly means that equation (4) used to compute the coefficients **a**(**x**) has multiple solutions, and therefore the functional (2) does not include sufficient constraints to guarantee a unique solution for the given nodal distribution. Based on this observation, for 2D, additional constraints are included in the functional (2) as

$$\bar{J}(\mathbf{x}) = \sum_{j=1}^{n} \left[ \left( u^h(\mathbf{x}_j) - u_j \right)^2 w\left( \|\mathbf{x} - \mathbf{x}_j\| \right) \right] + \mu_{x^2} a_{x^2}^2 + \mu_{xy} a_{xy}^2 + \mu_{y^2} a_{y^2}^2 \qquad (10)$$

where,

$$\boldsymbol{\mu} = \left[ \mu_{x^2} \;\; \mu_{xy} \;\; \mu_{y^2} \right] \qquad (11)$$

is defined as vector of positive weights for the additional constraints.

The choice of the additional constraints ensures that, when the classical MLS moment matrix is singular (multiple solutions), we favour the solution having the coefficients for the higher order monomials in the bases equal to zero. By choosing the weights for the additional constraints as small positive numbers we can ensure that the classical MLS solution is little changed when the moment matrix is not singular.

Using the same minimization procedure, the modified approximant is obtained as:

$$\overline{u}^h(\mathbf{x}) = \mathbf{P}^T(\mathbf{P}^T\mathbf{W}\mathbf{P} + \mathbf{H})^{-1}\mathbf{P}^T\mathbf{W}\mathbf{u} = \sum_{j=1}^{n} \overline{\emptyset}_j(\mathbf{x})u_j = \overline{\mathbf{\Phi}}^T(\mathbf{x})\mathbf{u} \qquad (12)$$

With the new shape function defined as

$$\overline{\mathbf{\Phi}}(\mathbf{x}) = \left[\, \overline{\emptyset}_1(\mathbf{x}) \;\ldots\; \overline{\emptyset}_n(\mathbf{x}) \,\right] = \mathbf{P}^T(\mathbf{P}^T\mathbf{W}\mathbf{P} + \mathbf{H})^{-1}\mathbf{P}^T\mathbf{W} \qquad (13)$$

Here, **H** is a matrix with all elements zeros except the last three diagonal entries, which are equal to **μ**

$$H = \begin{bmatrix} \mathbf{0}_{33} & \mathbf{0}_{33} \\ \mathbf{0}_{33} & diag(\boldsymbol{\mu}) \end{bmatrix} \qquad (14)$$

and the modified moment matrix is computed as:

$$\overline{\mathbf{M}} = \mathbf{P}^T\mathbf{W}\mathbf{P} + \mathbf{H} = \mathbf{M} + \mathbf{H} \qquad (15)$$

The small alteration of the moment matrix presented in the above equation is the only difference between the MMLS and the classic MLS with quadratic basis functions. Nevertheless, it can be shown that the nodal distributions which are admissible for the classical MLS with linear basis functions are also admissible for the presented MMLS [12].

## 3 Numerical Examples

### *3.1 Approximation capability in 2D*

To assess the approximations capability of the modified MLS shape functions with quadratic basis, it is compared with classical MLS shape function with linear and quadratic bases. A quartic spline weight function with circular domain was used in the definition of all shape functions:

$$w(s) = \begin{cases} 1 - 6s^2 + 8s^3 - 3s^4 & , \quad s \le 1 \\ 0 & , \quad s > 1 \end{cases} \qquad (16)$$

where *s* is the normalized distance

$$s_j = \frac{\|\mathbf{x} - \boldsymbol{x}_j\|}{R_j} \qquad (17)$$

and $R_j$ is the radius of the influence domain of node $\mathbf{x}_j$. In this example, the same weights for all the additional constraints ($\mu_x^2=\mu_{xy}=\mu_y^2=\mu$) and a constant radius of influence for all nodes ($R_j = R$) were used, as we used node distributions with constant nodal densities. A 2D rectangular problem domain was defined and the ge-

ometry was represented using both regular and irregular node distributions consisting of 324 nodes, as shown in Fig.1. The irregular nodal distribution consisted of uniformly scattered nodes were obtained by using the Matlab Halton sequence function [13]. The use of this function ensures a uniform nodal density for the problem domain. The following function was used for testing the approximation accuracy in 2D using MLS and the MMLS for different values of $\mu$ and $R$. The function was chosen to present a variety of behaviour in a surface which consists of Gaussian peaks with sharp descent.

$$u(x,y) = xe^{-x^2-y^2} \qquad (18)$$

The approximation accuracy was determined using the root mean square error evaluated using a regular distribution of N=81*81 points:

$$RMSE = \sqrt{\frac{\sum_{i=1}^{N}(u(x) - u^h(x))^2}{N}} \qquad (19)$$

The results are shown in Table1.

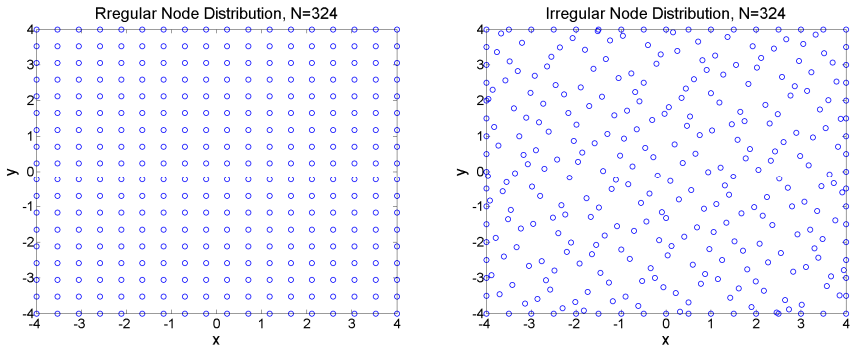


**(a)** **(b)**

**Figure 1.** a) Regular node distribution, b) Irregular node distribution.

**Table 1.** Root mean square error (RMSE) in approximating $\boldsymbol{u(x,y) = xe^{-x^2-y^2}}$ using 324 nodes with varying radius of nodal influence domain, R.

| **Approximation method** | **Regular node distribution** | | | **Irregular node distribution** | | |
|---|---|---|---|---|---|---|
| | **R=2.0** | **R=1.5** | **R=0.8** | **R=2.0** | **R=1.5** | **R=0.8** |
| MLS, linear BF | 0.0344 | 0.0272 | 0.0098 | 0.0361 | 0.0281 | 0.0118 |
| MLS, quadratic BF | 0.0081 | 0.0058 | Singular M | 0.0107 | 0.0080 | Singular M |
| MMLS, $\mu = 0.1$ | 0.0109 | 0.0106 | 0.0092 | 0.0131 | 0.0125 | 0.0113 |
| MMLS, $\mu = 0.01$ | 0.0083 | 0.0064 | 0.0064 | 0.0109 | 0.0085 | 0.0089 |
| MMLS, $\mu = 0.001$ | 0.0081 | 0.0059 | 0.0035 | 0.0107 | 0.0080 | 0.0053 |
| MMLS, $\mu = 0.0001$ | 0.0081 | 0.0058 | 0.0029 | 0.0107 | 0.0080 | 0.0046 |

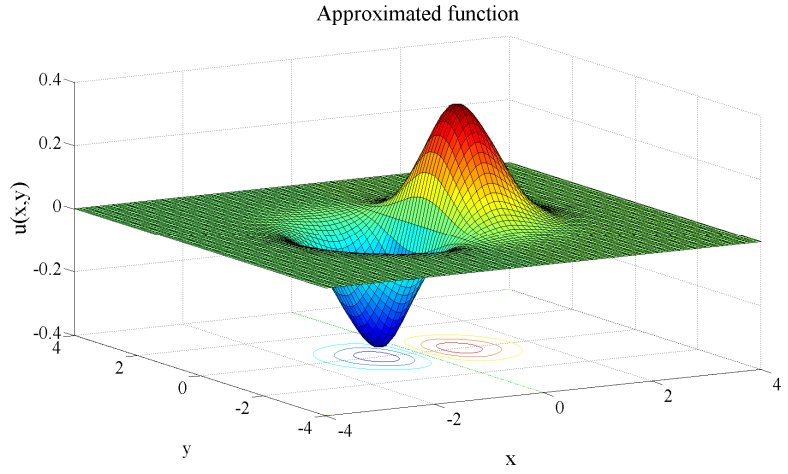


**Figure 2.** Approximated function by modified MLS (μ=0.1, R=0.8) using a regular distribution of 324 nodes.

From the results, it can be seen that as the nodal influence domain radius is gradually decreased, the classic MLS with quadratic basis fails due to singular moment matrix whereas the modified MLS with quadratic basis is stable. The approximation accuracy of MMLS is found to be better than that of classical MLS with linear basis function. Moreover, it is also evident that if the value of μ is decreased, the MMLS accuracy approaches the accuracy of classical MLS with quadratic basis function.

### *3.2 Applications in Biomechanics*

In brain biomechanics, for computing soft tissue deformation considering large deformation and large strain, Miller et al. [14] have developed an efficient finite element algorithm using total Lagrangian (TL) formulation and explicit time integration scheme. The algorithm is capable of handling both geometric and material nonlinearities. The adoption of TL formulation allows pre-computation of all derivatives with respect to spatial coordinates and the explicit time integration based on the central difference method eliminates the necessity for iterations during each time-step. These features resulted in significant reduction in the number of mathematical operations and constituted the base for real-time simulations. Several applications were developed in both surgical simulation and neuroimage registration based on this total Lagrangian explicit dynamics framework [15-19]. Motivated by the prospect of meshless method, Horton et al. [20] developed the Meshless Total Lagrangian Explicit Dynamics (MTLED) algorithm based on the earlier work of Miller et al. [14]. MTLED is based on the Galerkin weak form and uses a regular background grid for integration.

The modified MLS shape functions were incorporated in the MTLED algorithm. For easy imposition of the essential boundary conditions, a regularized weight function [21] was used which possesses almost interpolating properties, as shown in Fig 3.

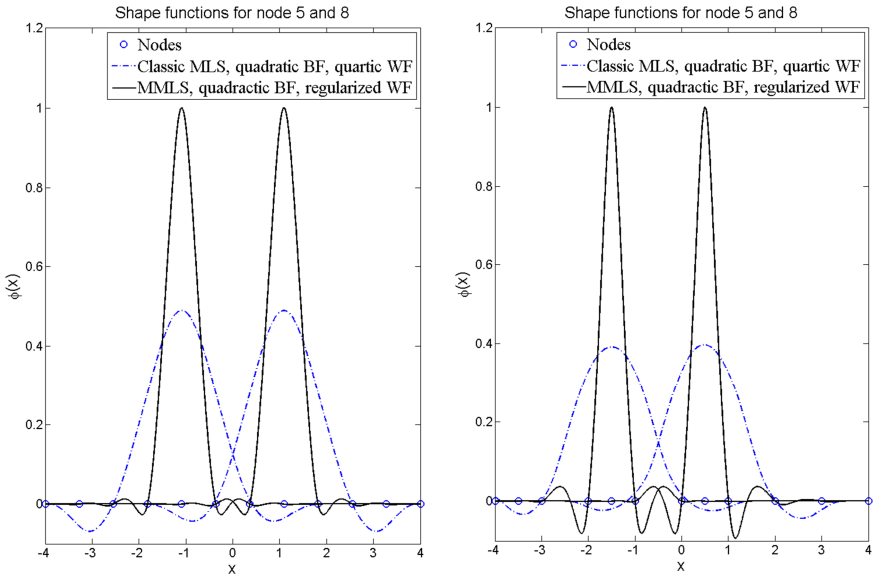


(a) (b)

**Figure 3.** Classic MLS and Modified MLS (μ = 0.01) with regularized weight function comparison, 12 nodes in 1-D, influence domain radius R = 3; a) regular, b) irregular nodal distributions.

Next, two cases of biomechanics applications, an extension of a soft tissue sample and craniotomy induced brain deformation are simulated using the meshless method which incorporates the MMLS with regularized weight functions. The results obtained by the meshless method are compared with those obtained using the commercial finite element software ABAQUS.

### *3.2.1 Extension of Soft Tissue Sample*

For the meshless computation of soft tissue extension, a 2D geometry (10cm x 4cm) was created and the domain and boundary were discretised using 57 nodes. To ensure integration accuracy, a regular background grid was used consisting of 1000 integration cells with one integration point per cell. For each node, the radius of the influence domain was constant ($R$ = 1.4). Loading in terms of displacement (3cm) was applied to the nodes on the right hand side boundary and the left boundary nodes were fixed. Explicit integration was performed using the central difference method, with mass proportional damping added (dynamic relaxation) to control the oscillations in order to reach the steady state solution [17, 22].

For simplicity, following [16, 17], the hyper-elastic Neo-Hookean material model was chosen in this numerical experiment to capture the behaviour of soft tissues undergoing large deformation. For the finite element analysis in ABAQUS, identical constitutive material laws, loading and boundary conditions were used; the steady state solution was obtained using the static solver with the default configuration. The simulation results and numerical details are presented in Fig.4 and Table 2.

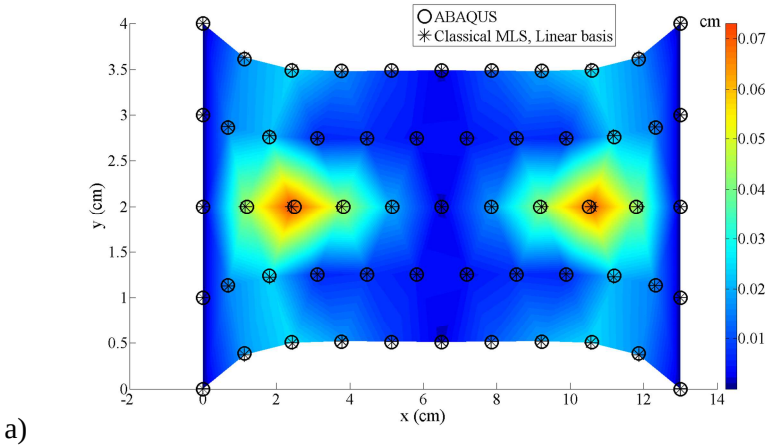


a)

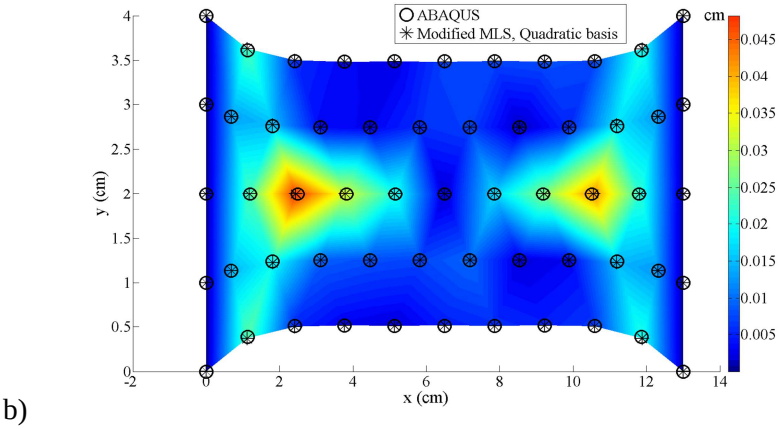


b)

**Figure 4.** Differences of the computed deformation field over the whole problem domain, a) between classic MLS (linear basis) and ABAQUS; b) between modified MLS and ABAQUS.

**Table 2.** Numerical details of comparison for the cases presented in Figure 4.

| Case | Nodes | Elements (ABAQUS) | Integration points (Meshless) | Average difference (mm) | Maximum difference (mm) |
|---|---|---|---|---|---|
| a) Classical MLS | 57 | 84 | 1000 | 0.14996 | 0.73014 |
| b) MMLS ($\mu=10^{-10}$) | 57 | 84 | 1000 | 0.10193 | 0.48192 |

For the given nodal influence domain radius, the classical MLS with quadratic basis failed due to the singularity of moment matrix. The differences in computed deformation fields over the whole problem domain are shown in Fig.4. The results in Table 2 shows that the maximum and average difference in displacements between MMLS and ABAQUS are lower compared to those between classic MLS with linear basis and ABAQUS.

### *3.3.3 Simulation of Brain Deformation in 2D*

In order to simulate brain deformation, based on experimental data [23] and previous modelling experience [18, 24], the Young's modulus for the brain parenchyma and the tumour was set to 3000 Pa and 6000 Pa respectively. Because of the fact that the brain tissue is almost incompressible [25], according to [24] a Poisson's ratio of 0.49 was assigned for both parenchyma and tumour. The ventricles are modelled as a cavity as the cerebrospinal fluid can freely move in and out of them. A variable load in terms of displacement was enforced on the nodes of the brain surface exposed by craniotomy. The interaction between skull and brain was modelled as finite sliding, frictionless contact and the skull was assumed to be rigid as it is orders of magnitude stiffer than the brain tissue. The brain model was discretised with 707 nodes, and for the meshless method 4988 integration points were created from a triangular background grid with four integration points per cell. A constant influence domain ($R$=8) and same weights for the additional constraints ($\mu = 10^{-7}$) were used in the meshless computation. Higher order plain strain elements with hybrid formulation were used in ABAQUS to handle the incompressibility of the soft tissues. The constitutive material laws, loading and boundary conditions were identical in both meshless and ABAQUS computations. The differences of the computed deformation field between classical MLS and modified MLS in comparison with ABAQUS are shown in Fig.5. Numerical details of the comparison are presented in Table 3.

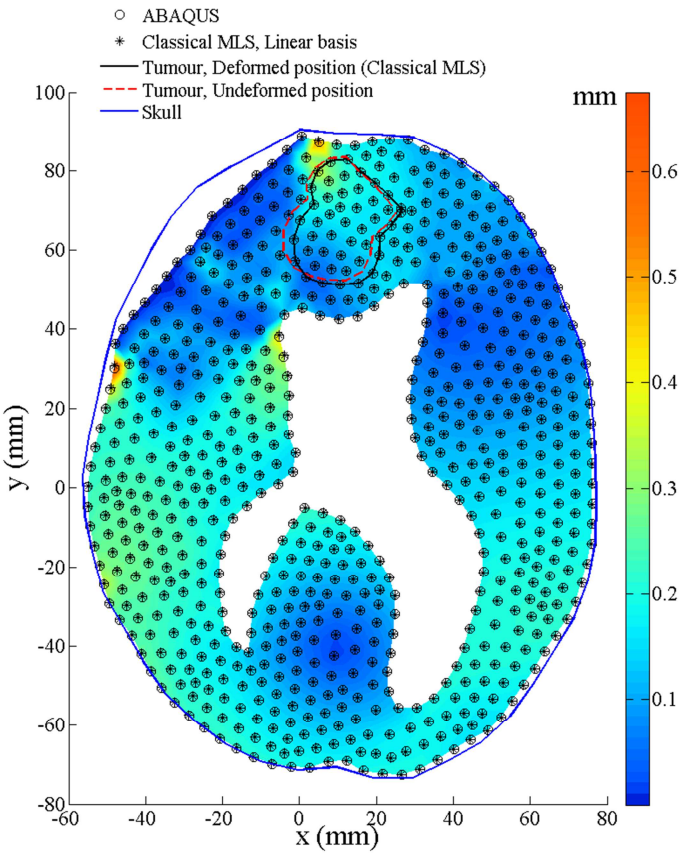
ABAQUS
Classical MLS, Linear basis
Tumour, Deformed position (Classical MLS)
Tumour, Undeformed position
Skull
mm
0.6
0.5
0.4
0.3
0.2
0.1
100
80
60
40
20
0
-20
-40
-60
-80
y (mm)
-60
-40
-20
0
20
40
60
80
x (mm)

(a)

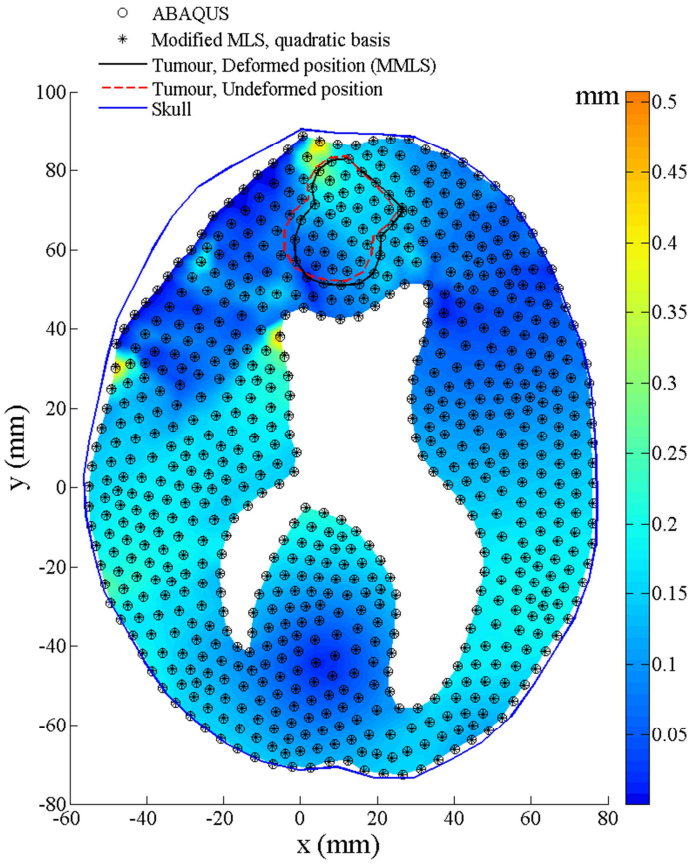


(b)

**Figure 5.** Differences of the computed deformation field in the brain a) between classic MLS (linear basis) and ABAQUS; b) between modified MLS and ABAQUS.

**Table 3.** Numerical details of comparison for the cases presented in Figure 5.

| Case | Nodes | Elements (ABAQUS) | Integration points (Meshless) | Average difference (mm) | Maximum difference (mm) |
|---|---|---|---|---|---|
| a) Classical MLS | 707 | 1247 | 4988 | 0.14509 | 0.67531 |
| b) MMLS ($\mu=10^{-7}$) | 707 | 1247 | 4988 | 0.12332 | 0.50729 |

In this experiment, for the given support domain radius, the classic MLS with quadratic basis also failed due to the singularity of moment matrix, whereas the modified MLS with quadratic basis had no problem in computing the shape functions. As shown in Table 3, the maximum and average differences between MMLS and ABAQUS are found to be lower compared to those between classic MLS with linear basis and ABAQUS.

## 4 Conclusions

In this paper we assessed the use of a modified MLS approximation with a meshless method for predicting soft tissue deformation. The approximation capability of the MMLS is evaluated against the classical MLS with linear and quadratic basis functions for a bivariate function. The results show that the MMLS approximation with a quadratic basis is stable with the same support domain size as the classical MLS using linear basis functions. Moreover, when the value of the weight $\mu$, associated with the additional constraints, is decreased, the accuracy of MMLS approaches the accuracy of classical MLS with quadratic basis functions.

A meshless method using the MMLS shape functions was used for the simulation of extension of a soft tissue sample and craniotomy induced brain deformation. A regularized weight function was used in these examples to enforce the essential boundary conditions. The results were compared with results obtained using the commercial finite element software ABAQUS. In both cases, the results indicate that the MMLS shape functions, having a quadratic basis, provide better accuracy with the same support domain size, compared to classical MLS with linear basis. With the same support domain size, classical MLS with quadratic basis simply fails due to singular moment matrices.

**Acknowledgments** The first author is a recipient of the SIRF scholarship and acknowledges the financial support of the University of Western Australia. The financial support of Australian Research Council (Discovery Grant No. DP120100402) and National Health and Medical Research Council (Grant No. APP1063986) is gratefully acknowledged.

### References

1. Cotin S, Delingette H, Ayache N: **A hybrid elastic model for real-time cutting, deformations, and force feedback for surgery training and simulation**. *Visual Comput* 2000, **16**(8):437-452.
2. Warfield SK, Talos F, Tei A, Bharatha A, Nabavi A, Ferrant M, Black PML, Jolesz FA, Kikinis R: **Real-time registration of volumetric brain MRI by biomechanical simulation of deformation during image guided neurosurgery**. *Computing and Visualization in Science* 2002, **5**(1):3-11.
3. Belytschko T, Lu YY, Gu L: **Element-Free Galerkin Methods**. *Int J Numer Meth Eng* 1994, **37**(2):229-256.
4. Liu G-R: **Meshfree methods: moving beyond the finite element method**: CRC press; 2010.
5. Wittek A, Joldes G, Miller K: **Algorithms for Computational Biomechanics of the Brain**. *Biol Med Phys Biomed* 2011:189-219.
6. Miller K, Wittek A, Joldes G: **Biomechanical Modeling of the Brain for Computer-Assisted Neurosurgery**. *Biol Med Phys Biomed* 2011:111-136.
7. Nayroles B, Touzot G, Villon P: **Generalizing the finite element method: Diffuse approximation and diffuse elements**. *Computational Mechanics* 1992, **10**(5):307-318.

8. Parks TW, Burrus CS: **Digital Filter Design**. New York: John Wiley & Sons, Inc.; 1987.
9. Nguyen VP, Rabczuk T, Bordas S, Duflot M: **Meshless methods: A review and computer implementation aspects**. *Mathematics and Computers in Simulation* 2008, **79**(3):763-813.
10. Lancaster P, Salkauskas K: **Surfaces Generated by Moving Least-Squares Methods**. *Math Comput* 1981, **37**(155):141-158.
11. Li S, Liu WK: **Meshfree Particle Methods**. Berlin: Springer-Verlag; 2004.
12. Joldes GR, Chowdhury HA, Wittek A, Doyle B, Miller K: **Modified Moving Least Squares with Polynomial Bases for Scattered Data Approximation**. UWA, Perth, WA; Report #ISML/02/2014; 2014 (school.mech.uwa.edu.au/ISML/index.php/Reports).
13. Fasshauer GE: **Meshfree Approximation Methods with MATLAB**: World Scientific Publishing Co., Inc. ; 2007.
14. Miller K, Joldes G, Lance D, Wittek A: **Total Lagrangian explicit dynamics finite element algorithm for computing soft tissue deformation**. *Communications in Numerical Methods in Engineering* 2006, **23**(2):121-134.
15. Wittek A, Joldes G, Couton M, Warfield SK, Miller K: **Patient-specific non-linear finite element modelling for predicting soft organ deformation in real-time; Application to non-rigid neuroimage registration**. *Prog Biophys Mol Bio* 2010, **103**(2-3):292-303.
16. Joldes GR, Wittek A, Miller K: **Suite of finite element algorithms for accurate computation of soft tissue deformation for surgical simulation**. *Med Image Anal* 2009, **13**(6):912-919.
17. Joldes GR, Wittek A, Miller K: **Computation of intra-operative brain shift using dynamic relaxation**. *Computer Methods in Applied Mechanics and Engineering* 2009, **198**(41-44):3313-3320.
18. Joldes GR, Wittek A, Couton M, Warfield SK, Miller K: **Real-Time Prediction of Brain Shift Using Nonlinear Finite Element Algorithms**. *Medical Image Computing and Computer-Assisted Intervention - Miccai 2009, Pt Ii, Proceedings* 2009, **5762**:300-307.
19. Joldes GR, Wittek A, Miller K: **Real-Time Nonlinear Finite Element Computations on GPU - Application to Neurosurgical Simulation**. *Comput Methods Appl Mech Eng* 2010, **199**(49-52):3305-3314.
20. Horton A, Wittek A, Joldes GR, Miller K: **A meshless Total Lagrangian explicit dynamics algorithm for surgical simulation**. *International Journal for Numerical Methods in Biomedical Engineering* 2010, **26**(8):977-998.
21. Most T, Bucher C: **A Moving Least Squares weighting function for the Element-free Galerkin Method which almost fulfills essential boundary conditions**. *Struct Eng Mech* 2005, **21**(3):315-332.
22. Joldes GR, Wittek A, Miller K: **An adaptive Dynamic Relaxation method for solving nonlinear finite element problems. Application to brain shift estimation.** *Int J Numer Method Biomed Eng* 2011, **27**(2):173-185.
23. Miller K, Chinzei K, Orssengo G, Bednarz P: **Mechanical properties of brain tissue in-vivo: experiment and computer simulation**. *Journal of biomechanics* 2000, **33**(11):1369-1376.
24. Zhang JY, Joldes GR, Wittek A, Miller K: **Patient-specific computational biomechanics of the brain without segmentation and meshing**. *Int j numer method biomed eng* 2013, **29**(2):293-308.
25. Miller K: **Biomechanics of the Brain**: Springer; 2011.